Integrated use of multispectral remote sensing and GIS for primary gold favorability mapping in Lahroud Region (NW Iran)

Solmaz Babakan[1*], Majid Mohammady Oskouei[2]

1- Phd Student at Sahand University of Technology
2- Mining Engineering Faculty, Sahand University of Technology, Tabriz, Iran

* Corresponding Author: s_babakan@sut.ac.ir

Received: 03 April 2013 / Accepted: 30 August 2014 / Published online: 07 September 2014

Abstract

In this study, the reliability of the primary gold mineralization exploration using multispectral ETM^+ imagery was investigated in Lahroud region, northwest Iran, which was conducted by integration of alteration and structural indicators. Co-occurrence of the clay minerals and iron oxides is an important criterion in gold deposit exploration; therefore, their alteration zones were mapped using Landsat 7 Enhanced Thematic Mapper Plus (ETM^+) data analysis by feature oriented component analysis (FPCS) and band ratio techniques considering their applicability and simplicity. The structural data layers including lithological units and faults maps were also utilized to enhance the accuracy of the results. The gold favorability map of the study area was then created by the combination of the aforementioned resultant alteration and structural data layers in ArcGIS based on the weights assigned by the analytic hierarchy process method (AHP) considering the main role of the alteration zones in gold mineralization exploration. The final primary gold favorability map was evaluated through the known Au indices and ore bodies in the study area. Quantitative assessment of the results was carried out by means of the frequency ratio coefficient (FRC) that normalizes the total number of Au signatures in each potential zone with the relevant area measurement. Approximately 16% of the study area was categorized as the most favorable zone for primary gold mineralization which involves 50% of the Au signatures. Accordingly, the high potential zone which represents the highest FRC value (3.14) confirms the efficiency and reliability of the applied procedure. Therefore, the application of multispectral remote sensing techniques alongside the structural analysis is a reliable, rapid and cost effective method for mineral exploration.

Keywords: Alteration mineral mapping; ETM^+; GIS; Multispectral data analysis; Analytic hierarchy process, Primary gold mineralization, Lahroud.

1–Introduction

Considering their remarkable extension, recognition of alteration haloes in mineral prospecting is an essential process and they have a key role in simplifying and prosperity of exploration programs. Despite the diverse techniques of the alteration mapping, developing remote sensing methods have found an increasing application in this arena and implementation of multispectral remote sensing techniques in ore deposits exploration has been intensively interested (Crosta and McM Moore, 1989; Loughlin, 1991; Zhang *et al.*, 2007b; Sadeghi *et al.*, 2013; Amer *et al.*, 2012).

Remote sensing sensors record spectral behavior of the materials comprising the earth's surface, and thus, they have been used for decades to map rock types, mineral assemblages and weathering characteristics. Remotely sensed data analysis, improving our abilities in the earth's surface recognition, is effective in arid/semi-arid regions where the geologic units are extensively exposed (Khan and Mahmood, 2008; Bedini, 2011; Zhang *et al*., 2007a).

Because of its suitable wavelength coverage, multispectral systems such as Landsat TM imagery have been routinely utilized in the detection of the ore deposit associated alteration zones, and as a result, it is considered as an efficient tool in mineral exploration, particularly in remote areas with little or no access (Zhang *et al*., 2007a).

Active tectonics of the study area and thus, extension of numerous igneous and metamorphic complexes in NW Iran has motivated plenty of systematic exploration programs and detailed investigations aiming economic mineralization in this area. The purpose of this study is to determine the most favorable areas of gold mineralization in Lahroud region, NW Iran, which confirms the efficiency of Landsat 7 Enhanced Thematic Mapper Plus (ETM^+) in gold mineralization potential mapping because of its ability in detection of related alteration minerals as well as its accessibility. Despite the higher spectral resolution of the Advanced Space borne Thermal Emission and Reflection Radiometer (ASTER) data, the indicator minerals of the gold mineralization including clay minerals and iron oxides are also detectable using ETM^+ images.

As gold cannot be detected directly by any remote sensing method, the presence of iron oxides alongside the clay minerals such as kaolinite, montmorillonite, and alunite could be used as an indicator for identification of hydrothermal alteration zones associated with gold mineralization considering their diagnostic spectral signatures in the visible/shortwave infrared portion of the electromagnetic spectrum (Kujjo, 2010; Zoheir and Emam, 2012). Hence, gold mineralization associated alteration minerals were mapped by the Feature oriented Principal Components analysis (FPCS) and band ratio techniques. These methods are practical and successfully employed in alteration mapping. At the same time, they are very simple methods leading to their popularity in the various researches. Moreover, structural features of the study area, including lithological units and faults maps were used for improving the reliability of the results. Finally, the gold potential map was generated by weighted overlaying of the aforementioned factor maps according to the weights assigned based on the analytic hierarchy process (AHP) method.

2– Study area

The study area is located at the NW Iran and the west of the Caspian Sea which covers approximately 4950 Km^2 of the boundary region of the East-Azerbaijan and Ardabil provinces as is shown in the figure 1. Coverage of the lithological units of the region is summarized in the table 1. As concluded from the table, igneous rocks are the most extended units in the study area.

Table 1) Coverage of the lithological units

Rock Type	**Area (Km^2)**	**(%)**
Residential Area or Landslide	11.77	0.24
Sedimentary	1908.92	38.45
Volcano-Sedimentary	306.74	6.18
Sedimentary-Metamorphic	20.43	0.41
Volcanic	2583.59	52.04
Volcanic-Metamorphic	10.39	0.21
Altered Zone	123.02	2.48

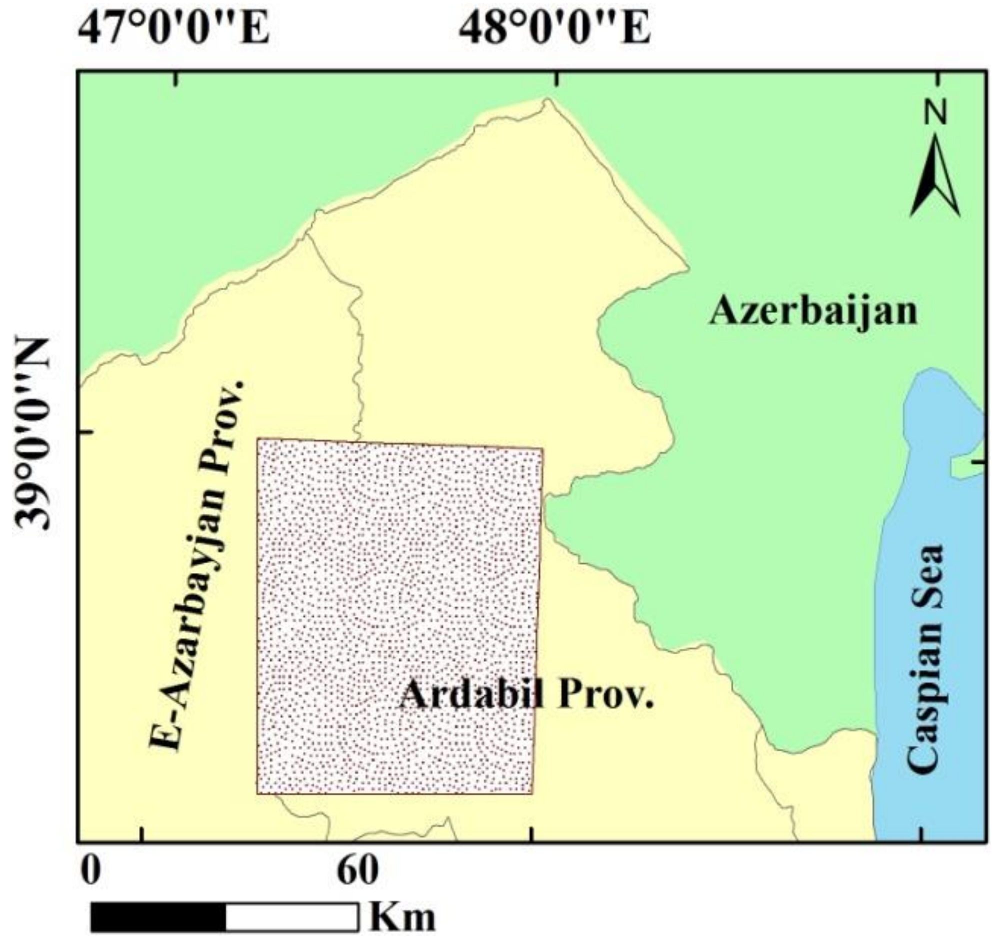

Figure 1) Location of the study area

3– Dataset

In this study, remotely sensed multispectral ETM^+ images acquired on June 5, 2000 were processed to extract alteration mineral zones associated with primary gold mineralization. Additionally, improving accuracy of the gold favorability map of the region, structural factor maps were utilized in the overlaying process.

Structural evaluation of the study area regards the ore formation was conducted using the lithological units and faults maps. Faults were digitized from the four 1:100,000 scale geologic quadrangle maps of Lahroud, Kaleybar, Meshkin Shahr and Ahar. Also, the 1:250,000 scale Ahar geologic map was used to extract lithological units of the region.

4– Pre-processing

Considering undesired interactions of the atmosphere and adjacent pixels, pre-processing is a necessary stage for improving clarity of the images and thus provides higher quality data for analysis purposes (Oskouei and Busch, 2008; Poormirzaee and Oskouei, 2010). One of the common atmospheric correction methods is to estimate the path radiance by the regression method and then to subtract this value from the signal received by the sensor (Mather and Koch, 2010).

In this study, the regression method was implemented for path radiance correction in which the scatter plot of the spectral bands against the thermal band (band 6) was plotted in turn and the intercept of the line best fitted to data points were subtracted from the corresponding band's digital numbers as the path radiance correction (PRC). This method supposes that the effect of the path radiance on the thermal bands is zero or negligible (Jiménez-Muñoz *et al*., 2010; Mather and Koch, 2010). The path radiance correction of ETM^+

bands is illustrated in table 2. As implied from the table, the path radiance decreases as the wavelength increases expectedly.

Table 1) PRC of ETM^+ bands

ETM^+ Bands	PRC	ETM^+ Bands	PRC
Band 1	44	Band 4	4
Band 2	25	Band 5	1
Band 3	8	Band 7	1

5– Methods

Image processing methods are aimed to increase the contrast between interesting targets and undesired background effects in the image (Camps-Valls *et al*., 2011). Digital processing of ETM^+ dataset was performed using ENVI 4.8 by the feature oriented component analysis and band ratio techniques.

5.1– Alteration indicators

5.1.1– Band ratio

Band ratioing is the common powerful satellite image processing technique, especially in areas where topographic effects are important. This method was widely applied in alteration mineral mapping. In fact, earth’s surface features have their particular spectral reflectance patterns in different wavelength portions which could be used as a kind of fingerprint of the objects. According to the position of the high reflectance and absorption spectral bands of the objects, the main concept of the band ratioing technique was developed (Wang and Nunez, 1992; Hadi and Najeeb, 2011; San *et al*., 2004; Fu *et al*., 2006; Zoheir and Emam, 2012; Beiranvand Pour *et al*., 2013; Rajendran *et al*., 2013).

The basic idea of the band ratio method is to emphasize the subtle variations in the spectral reflectance characteristics of the various surface covers or target objects. The important property of this method is its invariance to shading effects as the contribution of the geometric factor related to shading is approximately constant for all image bands; thus ratioing the two band values effectively cancels them out (Wang and Nunez, 1992; Hadi and Najeeb, 2011; San *et al*., 2004; Shalaby *et al*., 2010; Ranjbar *et al*., 2004; Fu *et al*., 2006).

Depending on the purpose of their application, e.g., lithology or alteration discrimination, lots of band ratios has been developed based on the spectral reflectance maxima and the position of the absorption features of the target minerals (Kujjo, 2010; Rajendran *et al*., 2013). The spectral bands of ETM^+ are well suited for recognition of the assemblages of the altered minerals.

A

B

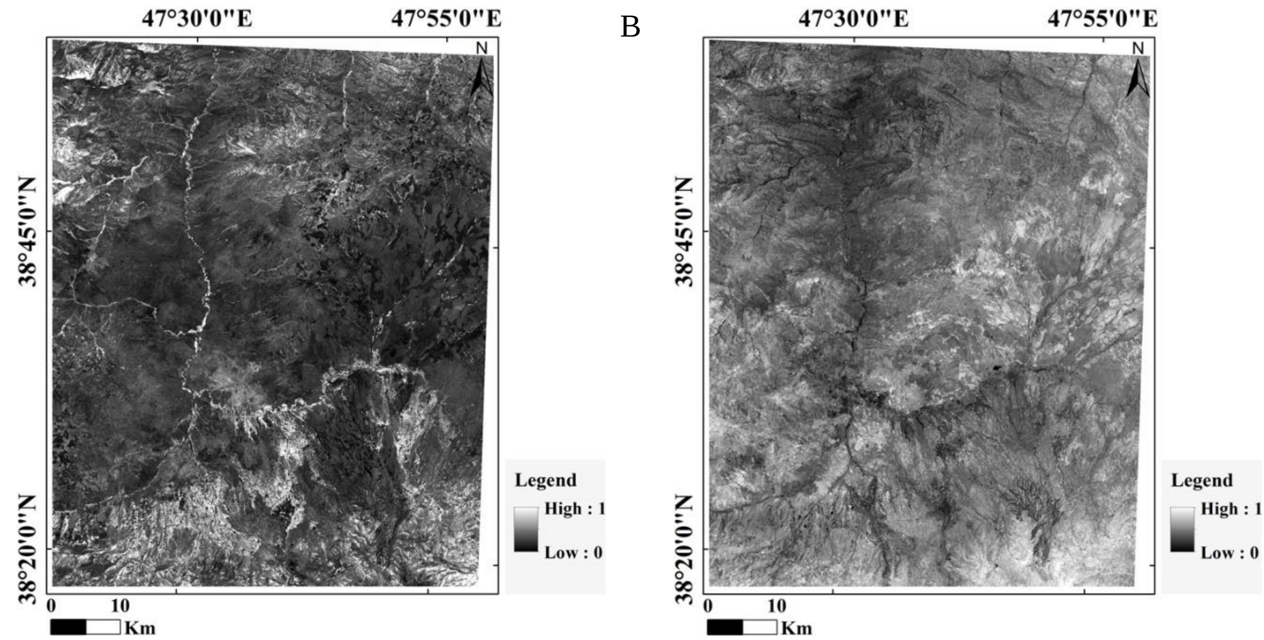

Figure 2) Normalized alteration maps by the band ratio method: A) clay mineral; B) iron oxides.

Generally, Landsat ETM+ band ratios 5/7 and 3/l were used to emphasize the clay and iron oxide alteration zones respectively (Dehnavi *et al*., 2010; Moghtaderi *et al*., 2007; van der Meer *et al*., 2012).

It is well established that the Landsat ETM+ band ratio 3/1 is efficient in Fe alteration mapping given their reflectance maxima and minima within the spectral range of bands 3 and 1 respectively, and thus increases the differences between the digital number of iron alteration zones and those of unaltered rocks leading to a better discrimination of hydrothermally altered and unaltered rocks (Dehnavi *et al*., 2010; Moghtaderi *et al*., 2007; Van der Meer *et al*., 2012; Sadeghi *et al*., 2013; Beiranvand Pour *et al*., 2013).

The most widespread products of the alteration process, hydroxyl minerals such as the clay minerals and sheet silicates, based on the position of band minima related to Al–OH vibrational absorption, have a diagnostic spectral absorption features in 2.1–2.4 μm (ETM+ band 7). At the same time they have a very high reflectance in the range of ETM+ band 5. Therefore, a band ratio of 5/7 would yield very high values for altered zones comprising dominantly hydroxyl-bearing minerals such as the clays, alunite, etc. (Ranjbar *et al*., 2004; Moghtaderi *et al*., 2007; Beiranvand Pour and Hashim, 2011; Van der Meer *et al*., 2012; Honarmand *et al*., 2011; Sadeghi *et al*., 2013; Beiranvand Pour *et al*., 2013).

Iron oxide and clay minerals alteration maps were produced by applying 3/1 and 5/7 band ratios respectively, and consequently normalized to be in the range of 0-1. The resultant alteration maps are presented in figure 2. Then, the product of the two alteration maps was calculated using the band math tool in the ENVI software which represents the simultaneous occurrence of the iron oxide and clay minerals by higher values. Finally, the region was categorized based on the probability of the gold mineralization, as the higher value the higher promising for Au mineralization. This categorized map was utilized in integration process of the factor maps to generate gold favorability map of the study area. The categorized favorability map of the primary gold mineralization based on the alteration indicators derived from the band ratio method is presented in the figure 3.

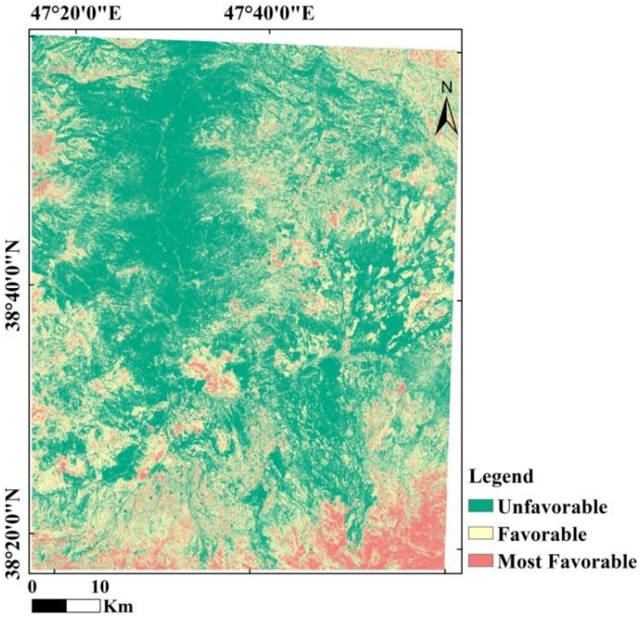

Figure 3) The categorized primary gold favorability map based on the alteration indicators derived from the band ratio method.

5.1.2– Features Oriented Component Analysis

Principal component analysis (PCA) is a mathematical procedure and a multivariate statistical technique widely applied in image processing to transform correlated spectral bands into a smaller number of uncorrelated spectral bands called principal components removing redundancy in the dataset. PCA helps to separate spectral signatures of the targets from the background, but it is not capable to eliminate topographic/atmospheric effects due to the fact that it is simply a rotation of spectral feature space to the maximum variance directions. This method has been intensively utilized for alteration mapping in metallogenic provinces (Ranjbar *et al*., 2004; Gabr *et al*., 2010; Rajendran *et al*., 2013).

Feature Oriented Principal Component Selection (FPCS) or Crosta technique is the selective PCA transform on the particular bands of the image believed to exhibit spectral information over the intended target objects (Crosta and McM Moore, 1989). Loughlin (1991) developed this method to map alteration zones by selecting specific Landsat TM band sets and applying PCA separately to them. So, the spectral information of the target alteration minerals was mapped into a single PC component despite the certain materials, e.g., vegetation. Identification of the principal components corresponding to the spectral information of the desired minerals, as well as the contribution of the original bands was performed through the analysis of the eigenvector values. Appropriate PC images were chosen by examining these loadings regards the spectral profile of the desired minerals (absorption and high reflectance bands). This technique was successfully implemented for mineral exploration purposes due to its ease of use and robustness, especially in areas with sparse or no vegetation coverage and considerable bedrock exposures (Crosta and Filaho, 2003; Mutua and Mibei, 2011; El Khidir and Babikir, 2013; Amuda *et al*., 2014; Poormirzaee *et al*., 2010; Vijdea *et al*., 2004; Kenea and Haenisch, 1996; Abedi *et al*., 2013). Loughlin used Landsat TM band sets comprising bands 1, 3, 4 and 5 or 7 and bands 1, 4, 5 and 7 to derive spectral information related to iron oxides and hydroxyl-bearing minerals like clays/carbonates respectively (El Khidir and Babikir, 2013; Amuda *et al*., 2014; Poormirzaee *et al*., 2010).

In this study, the Crosta technique was applied to ETM^+ bands 1, 3, 4, 5 and 1, 4, 5, 7 for mapping iron oxide and clay minerals respectively, and resulted principal components were examined regards the theoretical spectral profile (absorption/reflectance bands) of the target minerals. Eigenvalues and eigenvector loadings of both Crosta implementations are summarized in tables 3 and 4.

Table 2) FPCS for iron oxides using ETM^+ bands (1-3-4-7)

PCs	**PC1**	**PC2**	**PC3**	**PC4**
B1	0.37	0.05	0.39	0.84
B3	0.73	0.02	0.44	-0.52
B4	-0.06	-0.99	0.16	0.01
B7	0.58	-0.16	-0.79	0.12
Eigenvalues$^{\%}$	81.78	11.61	5.72	0.89

Table 3) FPCS for clay minerals using ETM^+ bands (1-4-5-7)

PCs	**PC1**	**PC2**	**PC3**	**PC4**
B1	0.34	-0.33	0.8	-0.37
B4	0.02	0.86	0.45	0.24
B5	0.65	0.35	-0.39	-0.55
B7	0.68	-0.19	-0.04	0.71
Eigenvalues$^{\%}$	76.23	16.64	5.94	1.2

According to the loadings of bands 1 (absorption) and 3 (reflectance) in table 3, as well as the loadings of bands 5 and 7 in table 4, anomalous desired alteration minerals were then highlighted by dark pixels in the corresponding 4^{th} PC components.

Similarly, generated gold mineralization associated alteration mineral maps by FPCS method were normalized to be in the range of 0-1 (figure 4) and their product map was calculated which presents co-occurrence of iron oxide and clay minerals, promising areas of Au mineralization, with high values. Thus, the region was categorized based on the probability of the gold mineralization. This categorized map was also utilized as a factor map in integration process to generate the gold favorability map of the study area. The categorized primary gold favorability map based on the alteration indicators derived from the FPCS method is represented in figure 5. This figure slightly differs from the results in the figure 3. However, most probable areas according to the both of the methods are consistent with the altered rock types from the available geological maps. Therefore, combination of their results would be more efficient in gold favorability mapping by considering all possible alteration zones.

A

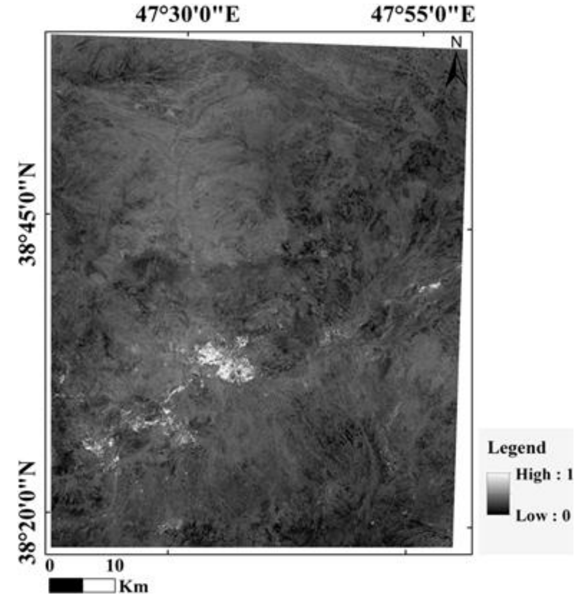

B

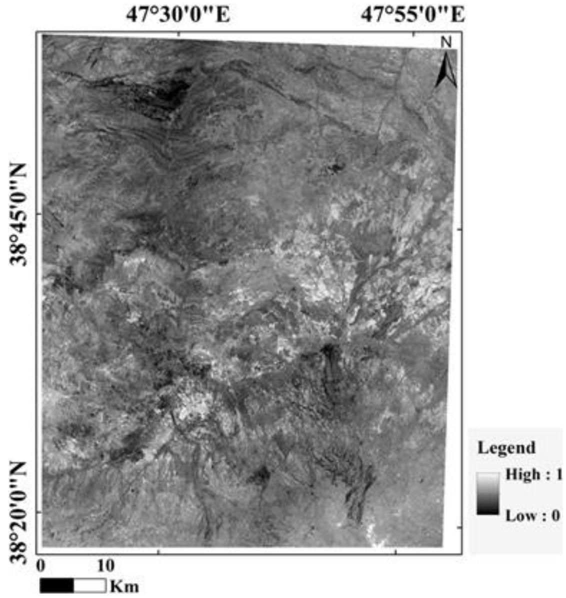

Figure 4) Normalized alteration maps by FPCS method A) clay mineral B) Iron oxides.

Table 5) Structural characteristics of the gold deposits in the world and NW Iran.

Gold Mine	**Location**	**Structural characteristics**
Grasberg Mine (Pollard et al., 2005) (world's lowest-cost, largest Au-Cu producer)	Indonesia, Papua province	Hosted within the Grasberg Igneous Complex, formed in a left-lateral strike-slip fault system.
Poplar Mountain gold deposit (Chi *et al*., 2008)	Canada, western New Brunswick province	Hosted in the Poplar Mountain volcanic complex (PMVC), located along the regional Woodstock fault zone.
Musselwhite Mine and Hammond Reef (Maura and Louise, 2011)	Canada, Ontario provinces	Shear-zone-hosted gold deposits hosted in the metamorphic rocks.
The Fazenda Brasileiro mine (Reinhardt and Davison, 1990)	Brazil, Bahia State, Rio Itapicuru greenstone belt	A hydrothermal quartz-gold vein deposit, hosted by iron-rich chlorite-magnetite schists, associated with shear zones.
Goldfield belt of the Piranshahr-Sardasht-Saqez zone (consists of several orogenic gold deposits/ occurrences including the Qolqoleh (the most significant mineralization), Kervian, Qabaqloujeh, Kharapeh, Alut, Hamzeh–Gharanein)	The northern part of the Sanandaj-Sirjan metamorphic zone	Associated with shear zones located within or adjacent to the major Saqez–Sardasht thrust fault and other confining normal faults. Qolqoleh gold deposit: hosted by mafic to intermediate meta-volcanic/sedimentary rocks (Afzal *et al*., 2013; Aliyari *et al*., 2011; Aliyari *et al*., 2007). Kervian gold deposit: located in greenschist facies metamorphic complex (Heidari *et al*., 2008).
Chah-Bagh gold occurrence (Muteh Mining District with ten gold deposits and occurrences)	The central part of the Sanandaj-Sirjan metamorphosed zone of the Zagros orogenic belt	Muteh Mining District: hosted by schist-gneiss, subsidiary amphibolite- quartzite and intruded by leucogranites, controlled by NW normal faults and joints (Moritz *et al*., 2006). Chah-Bagh gold mineralization: localized in shear zones, hosted by the NE-SW trending metamorphosed volcanic and volcano-sedimentary rocks (Kouhestani *et al*., 2008).
Sari Gunay epithermal gold deposit (Richards *et al*., 2006; Mahmoodi *et al*., 2012)	South-east of the Kordistan province	Located at the Ghorveh-Bijar belt (located between and sub-parallel to the Sanandaj-Sirjan metamorphic belt and the Orumieh-Dokhtar volcanic belt) of NW–SE trending structurally controlled volcanics.

5.2– Structural indicators

The main gold deposits in the world have been controlled by structural factors and thus the combination of the structural indicators such as the lithology and faults maps with alteration indicators would be helpful in gold mineralization mapping. Some examples of the world gold deposits as well as the known gold deposits in the NW Iran and their structural characteristics are summarized in table 5. A review on the known gold deposits in the world and especially around the study area indicates that lithological units, including metamorphic and igneous rocks as well as the structural shear zones or highly fractured areas are efficient indicators of the high probability of gold mineralization.

For investigation of the structural characteristics of the region regards the gold mineralization, faults map was generated by digitizing related 1:100,000 geologic maps covering the study area: Ahar, Kaleybar, Lahroud and Meshkin Shahr. The Euclidian distance from the faults was then created by ArcGIS and practiced as a weighted factor map. For this purpose, the resultant distance map was normalized between 0-1 and subtracted from one. So, the weights were decreased as the distance from the faults was increased. The lithological units of the study area were extracted from the 1:250,000 scale Ahar geologic map and weighted based on the main rock types described in table 1. Lithological units and faults extension at the study area are presented in figure 6.

6– Combination of results

Integrating remotely sensed data with structural characteristic of the study area provides the opportunity of identifying the location of the favorite areas for mineral deposits (Durning *et al*., 1998). GIS can easily produce mineral favorability maps by integrating the results of different investigations such as geological, geophysical and geochemical studies. Using a powerful weighting method, GIS provides a better prediction on the mineralization potential (Poormirzaee and Oskouei, 2010).

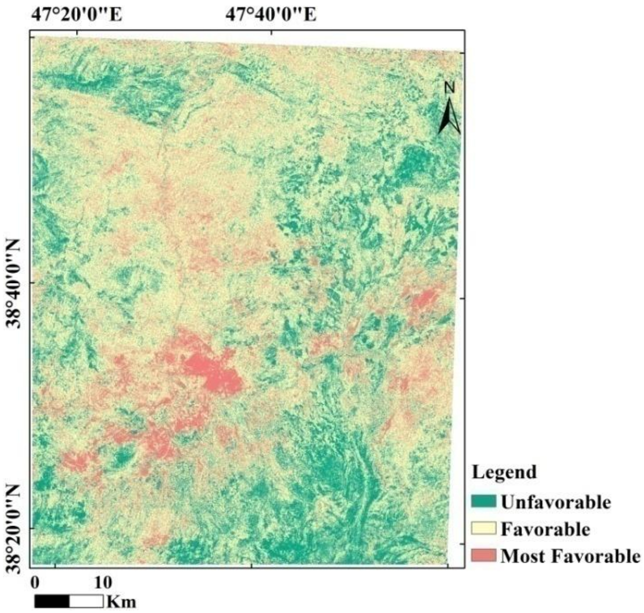

Figure 5) The categorized primary gold favorability map based on the alteration indicators derived from the FPCS method.

Thus, indicator factor maps were integrated in ArcGIS desktop through weighted overlay to improve the precision and accuracy of the gold favorability map. These factor maps were overlaid according to the weights assigned based on the AHP method considering their relative importance in the gold mineralization mapping. So, the alteration maps were given higher weights in comparison to the structural maps because of their importance in economic ore body recognition. In fact, the simultaneous occurrence of the clay minerals and iron oxides is an essential criterion for gold mineralization exploration by remote sensing techniques. Both of the alteration maps from band ratio and FPCS techniques were equally weighted due to their similar importance.

In the case of structural factors, higher weight was assigned to the faults considering the stronger relation of the primary gold mineralization with hydrothermal processes and fault systems. The weights assigned for the factor maps and their categories are shown in table 6. The resulted gold potential map was categorized and validated based on the 10 known Au indices and ore bodies in the study area. The final gold favorability map of the study area is represented in figure 7. The known Au signatures extracted from National Geosciences Database of Iran (www.ngdir.com) are also remarked on the final gold favorability map.

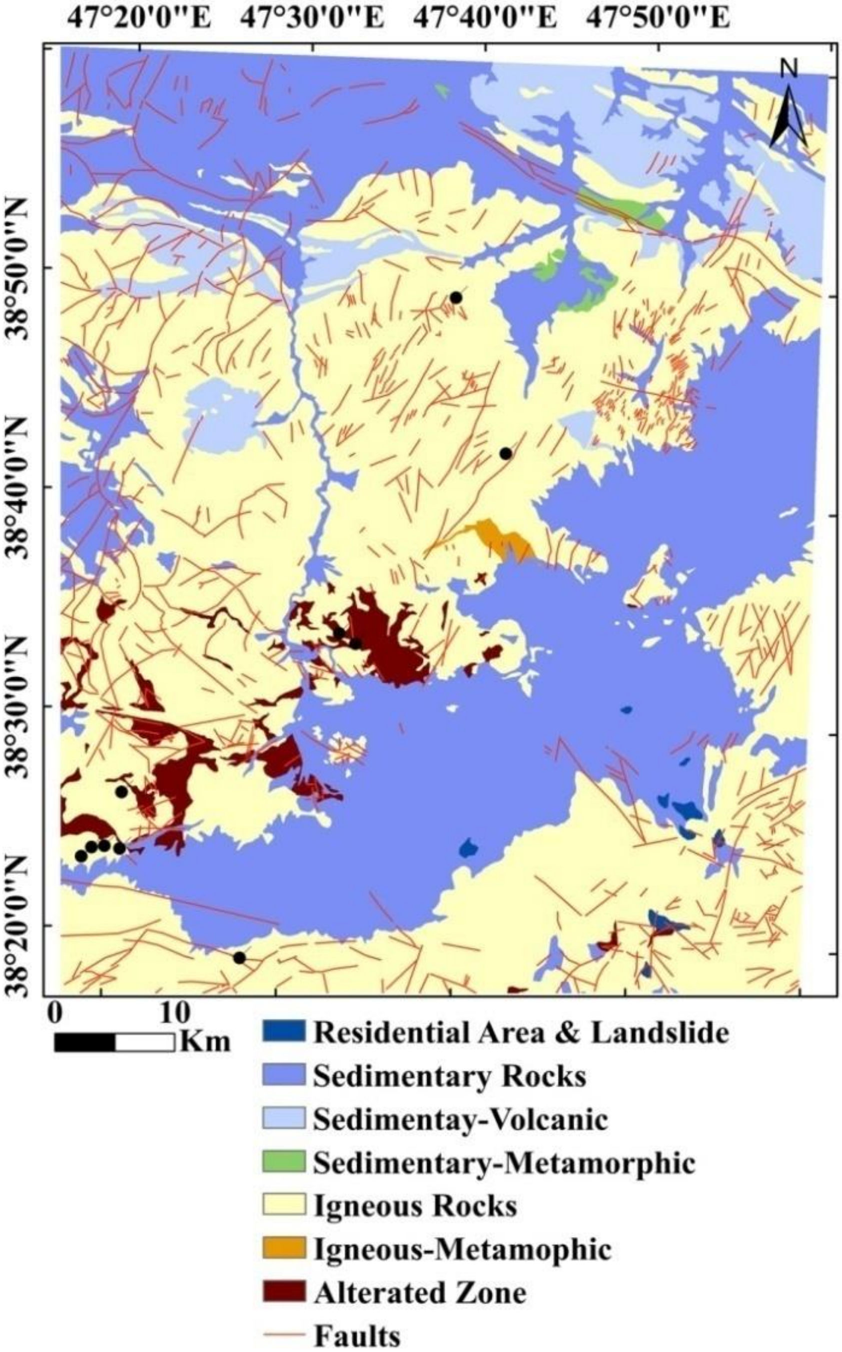

Figure 6) Lithological units and faults extension at the study area.

7– Validation of results

The known Au indices and ore bodies in the study area were utilized to examine the accuracy of the applied method for gold exploration which were extracted from the national geosciences database of Iran site for Ahar, Kaleybar, Lahroud, Meshkin Shahr sheets at the scale of 1:100,000. As implied from the final map (figure 7), determined potentials are strongly coinciding the previously found Au indices. Quantitative assessment of the results is also illustrated in table 7. This table presents the total number of known Au indices and ore bodies in different gold potential zones.

Table 6) Weights of the factor maps assigned by AHP method.

	Factor Maps	Weights	Classes	Scores
Structural Factors	Fault Map	22%	<760.47	1
			760.47-1749.91	3
			1749.91-3067.96	5
			3067.96-4716.64	7
			>4716.64	9
	Lithological outcrops	14%	Residential Area or Landslide	1
			Sedimentary	4
			Volcano-sedimentary	5
			Sedimentary-Metamorphic	6
			Volcanic	7
			Volcanic-Metamorphic	8
			Altered Zone	9
Alteration Factors	Band Ratio Alteration Map	32%	Low	1
			Medium	5
			High	9
	FPCS Alteration Map	32%	Low	1
			Medium	5
			High	9

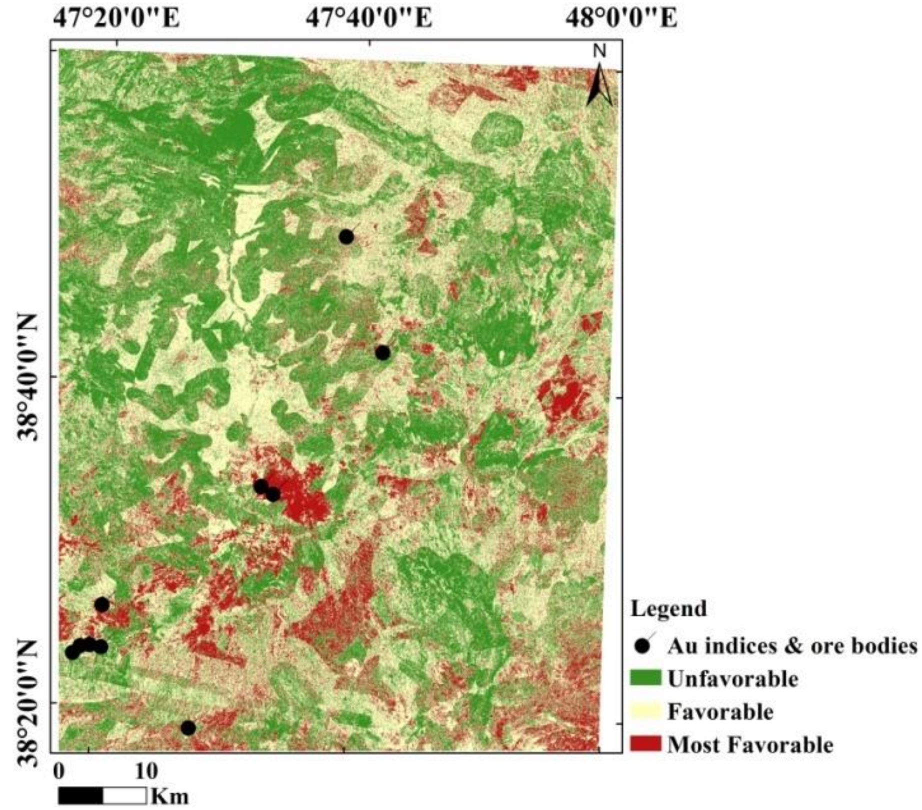

Figure 7) Final gold favorability map alongside the known Au indices and ore bodies at the study area.

The last column indicates the frequency ratio coefficient (FRC) that normalizes this number with each zone's area measurement. As implied from the table, the FRC for the high potential zone is considerably high and thus emphatically confirms high performance of the proposed method for gold mineralization potential mapping.

Table 4) Quantitative assessment of the results of Au potential mapping.

Au Potential	Number of indices and ore bodies	Coverage (Km^2)	FRC ($Number^{\%}/Coverage^{\%}$)
Unfavorable	2	1890.33	0.52
Favorable	3	2271.35	0.65
Most Favorable	5	788.43	3.14

8– Conclusions

Current paper was aimed to present the efficiency of multispectral ETM^+ imagery in primary gold mineralization exploration which was conducted by integration of different data layers from different sources. Alteration maps extracted by band ratio and FPCS methods were combined with the structural data layers including lithological units and faults maps in ArcGIS environment, according to the weights assigned by the AHP method based on their relative importance in gold mineralization. The final gold potential map was validated using the location of known Au indices and ore bodies indicating the high performance of the proposed procedure and representing the overall trend of mineralization in the field. Therefore, the application of multispectral remote sensing techniques in conjunction with the structural analysis is a reliable method for mineral exploration. As well, it is rapid and cost effective in comparison to the other exploration methods.

Acknowledgments:

The authors would like to thank Prof. A. Madani and Dr. B. Sadeghi for their appreciate comments which help us to improve manuscript.

References:

Abedi, M., Gholami, A., Norouzi, G.H. 2013. A stable downward continuation of airborne magnetic data: A case study for mineral prospectivity mapping in Central Iran. Computers and Geosciences: 52, 269–280.

Afzal, P., Dadashzadeh Ahari, H., Rashidnejad Omran, N., Aliyari, F. 2013. Delineation of gold mineralised zones using concentration–volume fractal model in Qolqoleh gold deposit, NW Iran. Ore Geology Reviews: 55, 125–133.

Aliyari, F., Rastad, E., Mohajjel, M. 2011. Gold deposits in the Sanandaj–Sirjan zone orogenic gold deposits or intrusion-related gold systems. Resource Geology: 62, 296–315.

Aliyari, F., Rastad, E., Zengqian, H. 2007. Orogenic gold mineralization in the Qolqoleh deposit, northwestern Iran. Resource Geology: 57, 269–282.

Amer, R., Kusky, T., El Mezayen, A. 2012. Remote sensing detection of gold related alteration zones in Um Rus area, Central Eastern Desert of Egypt. Advances in Space Research: 49, 121–134.

Amuda, A. K., Danbatta, U. A., Najime, T. 2014. Utilisation of Landsat 7 ETM^+ multispectral data and ASTERGDEM in geological investigation and alteration mapping around Yankara-Dan Sabo-Takulawa area within Wonaka Schist Belt, northwestern Nigeria. Journal of Environmental and Earth Sciences: 4, 44–56.

Bedini, E. 2011. Mineral mapping in the Kap Simpson Complex, central east Greenland, using HyMap and ASTER remote sensing data. Advances in Space Research: 47, 60–73.

Beiranvand Pour, A., Hashim, M. 2011. Application of advanced spaceborne thermal emission and reflection radiometer (ASTER) data in geological mapping. International Journal of Physical Sciences: 6, 7657–7668.

Beiranvand Pour, A., Hashim, M., van Genderen, J. 2013. Detection of hydrothermal alteration zones in a tropical region using satellite remote sensing data: Bau goldfield, Sarawak, Malaysia. Ore Geology Reviews: 54, 181–196.

Camps-Valls, G., Benediktsson, J. A., Bruzzone, L., Chanussot, J. 2011. Introduction to the Issue on Advances in

Remote Sensing Image Processing. IEEE Journal of Selected Topics in Signal Processing: 5, 365–369.

Chi, G., Watters, S., Davis, W. J., Ni, P., Castonguay, S., Hoy, D. 2008. Geologic, geochemical, and geochronological constraints on the genesis of gold mineralization at Poplar Mountain, Western New Brunswick, Canada. Exploration and Mining Geology: 17, 101–130.

Crosta, A. P., Filaho, C. R. 2003. Targeting key alteration minerals in epithermal deposits in Patagonia, Argentina, using ASTER imagery and principal component analysis. International Journal of Remote Sensing: 24, 4233–4240.

Crosta, A. P., McM Moore, J. 1989. Enhancement of Landsat Thematic Mapper imagery for residual soil mapping in SW Minais Gerrain. In Proc. 7th (ERIM) Thematic Conference: Remote Sensing for Exploration Geology, Calgary, Alberta, Canada, 2-6 October, 1173–1187.

Dehnavi, A. G., Sarikhani, R., Nagaraju, D. 2010. Image processing and analysis of mapping alteration zones in environmental research, east of Kurdistan, Iran. World Applied Sciences Journal: 11, 278–283.

Durning, W. P., Polis, S. R., Frost, E. G., Kaiser, J. V. 1998. Integrated use of remote sensing and GIS for mineral exploration: A Project of the NASA Affiliated Research Center at San Diego State University. Affiliated Research Center Final Report. Series ARC-SDSU-002-97.

El Khidir, S. O., Babikir, I. A. A. 2013. Digital image processing and geospatial analysis of Landsat 7 ETM+ for mineral exploration, Abidiya area, North Sudan. International Journal of Geomatics and Geosciences: 3, 645–658.

Fu, Z. Y., Caelli, T. M., Liu, N. J., Robles Kelly, A. 2006. Boosted band ratio feature selection for hyperspectral image classification. in 18th International Conference on Pattern Recognition (ICPR), Hong Kong, China, 20-24 August, 1059-1062. doi: 10.1109/ICPR.2006.334.

Gabr, S., Ghulam, A., Kusky, T. 2010. Detecting areas of high-potential gold mineralization using ASTER data. Ore Geology Reviews: 38, 59–69.

Hadi, G. S., Najeeb, A. A. Z. 2011. Using the band ratio classification method to detect the regions that need to remove sedimentation in Tigris River. Iraqi Journal of Science: 52, 376–380.

Heidari, S. M., Rastad, E., Mohajel, M. 2008. Kervian orogenic gold deposit in northwest of Iran. in 33rd International geological congress (IGC), Oslo, Norway, 6-14 August.

Honarmand, M., Ranjbar, H., Shahabpour, J. 2011. Application of spectral analysis in mapping hydrothermal alteration of the northwestern part of the Kerman Cenozoic Magmatic Arc, Iran. Journal of Sciences, Islamic Republic of Iran: 22, 221–238.

Jiménez-Muñoz, J. C., Sobrino, J. A., Mattar, C., Franch, B. 2010. Atmospheric correction of optical imagery from MODIS and Reanalysis atmospheric products. Remote Sensing of Environment: 114, 2195–2210. Kenea, N. H., Haenisch, H. 1996. Principal component analyses for lithologic and alteration mappings: examples from the Red Sea Hills, Sudan. International Archives of Photogrammetry and Remote Sensing: 31, part B7, 271–275.

Khan, S. D., Mahmood, K. 2008. The application of remote sensing techniques to the study of ophiolites. Earth-Science Reviews: 89, 135–143.

Kouhestani, H., Rastad, E., Rashidnejad Omran, N. 2008. Auriferous sulfides from the Chah-Bagh Gold Occurrence, Muteh Mining District. Journal of Sciences of the Islamic Republic of Iran: 19, 125–136.

Kujjo, C. P. 2010. Application of remote sensing for gold exploration in the Numba Mountains, Sudan. MSc Dissertation, College of Bowling Green State Univ. Geology, 110 p.

Loughlin, W. P. 1991. Principal component analysis for alteration mapping. in Proc. 8th Thematic Conference on Geologic Remote Sensing, Denver, Co., U.S.A., 29 April-2 May, 293–306.

Mahmoodi, O., Asadi Harouni, H., Norouzi, Gh. 2012. Using ETM^+ data to determine altered zones in Sari Gunay Gold Deposit, Kordestan. in 1st Iranian Mining Technologies Conference and Exhibition (IMT2012), Yazd, Iran, 5-7 September, 276–283.

Mather, P. M., Koch, M. 2010. Preprocessing of remotely-sensed data, in: Computer processing of remotely-sensed images: an introduction. fourth ed. New York, Wiley, pp. 87–125.

Maura, K., Louise, H. M. 2011. Microstructural control of gold mineralization in shear–zone-hosted gold deposits: examples from the superior province of northwestern Ontario. in Proc. Northeastern (46th Annual) and North-Central (45th Annual) Joint Meeting, Pittburgh, Pennsylvania, U.S.A., 20–22 March. doi: 10.2113/gsecongeo. 85.5.952.

Moghtaderi, A., Moore, F., Mohammadzadeh, A. 2007. The application of advanced space-borne thermal emission and reflection (ASTER) radiometer data in the detection of alteration in the Chadormalu paleocrater, Bafq region, Central Iran. Journal of Asian Earth Sciences: 30, 238–252.

Moritz, R., Ghazban, F., Singer, B. S. 2006. Eocene gold ore formation at Muteh, Sanandaj-Sirjan tectonic zone, western Iran: a result of late-stage extension and exhumation of metamorphic basement rocks within the Zagros Orogen. Economic Geology: 101, 1497–1524.

Mutua, J., Mibei, G. 2011. Remote sensing application in geothermal exploration: case study of Barrier Volcanic Complex, Kenya. Geothermal Resources Council Transactions: 35, 943–947.

Oskouei, M. M., Busch, W. 2008. A geostatistically based preprocessing algorithm for hyperspectral data analysis. GIScience and Remote Sensing: 45, 356–368.

Pollard, P. J., Taylor, R. G., Peters, L. 2005. Ages of intrusion, alteration and mineralization at the Grasberg Cu-Au deposit, Papua, Indonesia. Economic Geology: 100, 1005–1020.

Poormirzaee, R., Mohamadzade, M. J., Naseri, A., Zekri, H. 2010. Interpretation and Processing of ETM+ Data for Alteration Mapping, A Case Study: Behabad, Iran. in Proc. 5th IASME/ WSEAS, International Conference on Water Resources, Hydraulics and Hydrology (WHH'10), Proc. of the 4th IASME/WSEAS, International Conference on Geology and Seismology (GES '10), University of Cambridge, UK, 23-25 February.

Poormirzaee, R., Oskouei, M. M. 2010. Use of spectral analysis for detection of alterations in ETM data, Yazd, Iran. Applied Geomatics: 2, 147–154.

Rajendran, S., Nasir, S., Kusky, T. M., Ghulam, A., Gabr, S., El-Ghali, M. A. K. 2013. Detection of hydrothermal mineralized zones associated with listwaenites in Central Oman using ASTER data. Ore Geology Reviews: 53, 470–488.

Ranjbar, H., Honarmand, M., Moezifar, Z. 2004. Application of the Crosta technique for porphyry copper alteration mapping, using ETM^+ data in the southern part of the Iranian volcanic sedimentary belt. Journal of Asian Earth Sciences: 24, 237–243.

Reinhardt, M. C., Davison, I. 1990. Structural and lithologic controls on gold deposition in the shear zone-hosted Fazenda Brasileiro Mine, Bahia State, Northeast Brazil. Economic Geology: 85, 952–967.

Richards, J. P., Wilkinson, D., Ullrich, T. 2006. Geology of the sari gunay epithermal gold deposit, northwest Iran. Economic Geology: 101, 1455–1496.

Sadeghi, B., Khalajmasoumi, M., Afzal, P., Moarefvand, P., Yarebi, A.B., Wetherelt, A., Foster, P., Ziazarifi, A. 2013. Using ETM+ and ASTER sensors to identify iron occurrences in the Esfordi 1:100,000 mapping sheet of Central Iran. Journal of African Earth Sciences: 85, 103–114.

San, B. T., Sumer, E. O., Gurcay, B. 2004. Comparison of band ratioing and spectral indices methods for detecting alunite and kaolinite minerals using aster data in Biga region, Turkey, in Proc. 20th ISPRS Congress: 35, Part B7, Technical Commission VII, Istanbul, Turkey, 12-23 July.

Shalaby, M. H., Bishta, A. Z., Roz, M. E., El Zalaky, M. A. 2010. Integration of geologic and remote sensing studies for the discovery of uranium mineralization in some granite plutons, Eastern Desert, Egypt. Journal of King Abdulaziz University: Earth Sciences: 21, 1–25.

van der Meer, F. D., van der Werff, H. M. A., van Ruitenbeek, F. J. A., Hecker, C. A., Bakker, W. H., Noomen, M. F., van der

Meijde, M., Carranza, E. J. M., de Smeth, J. B., Woldai, T. 2012. Multi-and hyperspectral geologic remote sensing: a review. International Journal of Applied Earth Observation and Geoinformation: 14, 112–128.

Vijdea, A. M., Sommer, S., Mehl, W. 2004. Use of remote sensing for mapping and evaluation of mining waste anomalies at national to multi-country scale, A case study to integrate remote sensing information with thematic data layers and national inventories on mining features in pre-accession countries. Joint Research Centre of the European Commission, Ispra, EUR 21185 EN.

Wang, G., Nunez, M. 1992. A new method of estimating path radiance for band ratio application. International Journal of Remote Sensing: 13, 527–539.

Zhang, X., Pazner, M., Duke, N. 2007. Lithologic and mineral information extraction for gold exploration using ASTER data in the south Chocolate Mountains (California). ISPRS Journal of Photogrammetry and Remote Sensing: 62, 271–282.

Zhang, Y., Yang, J., Yao, F. 2007. The potentials of multi-spectral remote sensing techniques for mineral prognostication - taking Mongolian Oyu Tolgoi Cu-Au deposit as an example. Earth Science Frontiers: 14, 63–69.

Zoheir, B., Emam A. 2012. Integrating geologic and satellite imagery data for high-resolution mapping and gold exploration targets in the South Eastern Desert, Egypt. Journal of African Earth Sciences: 66–67, 22–34.